Biomedicine & Pharmacotherapy 107 (2018) 359–367

Contents lists available at ScienceDirect

Biomedicine & Pharmacotherapy

journal homepage: www.elsevier.com/locate/biopha

MiR-148b-3p inhibits renal carcinoma cell growth and pro-angiogenic phenotype of endothelial cell potentially by modulating FGF2

Hui Zhang[a,1], Qing Ye[b,*,1], Zhenfang Du[a], Min Huang[a], Ming Zhang[a], Huifeng Tan[a]

[a] Department of Nephropathy, Zhangjiagang Hospital of Traditional Chinese Medicine, Zhangjiagang, Jiangsu Province, China
[b] Department of Nephropathy, Shanghai Corps Hospital of Chinese People's Armed Police, Sahnghai, China

ARTICLE INFO

Keywords:
MiR-148b-3
Renal carcinoma
Invasion
Tube formation
FGF2

ABSTRACT

MicroRNAs (miRNAs) have been implicated in a large number of biological processes such as tumor angiogenesis. MiR-148b-3p has been identified as a tumor suppressor in multiple cancer types and the function of miR-148b-3p in renal carcinoma remains unidentified. In this study, we found that the expression of miR-148b-3p was decreased in renal carcinoma based on GEO analysis and the gain-of-function experiments revealed that miR-148b-3p promoted renal carcinoma cell apoptosis and suppressed cell proliferation, migration *in vitro* and tumor growth *in vivo*. Functionally, the tube formation, invasion and migration capabilities of human umbilical vein endothelial cells (HUVECs) were suppressed by conditioned media derived from renal carcinoma 786-O cells that were transfected with miR-148b-3p mimics. Meanwhile, these conditioned media inhibited the proliferation and promoted apoptosis of HUVECs. The key angiogenesis inducer hypoxia inducible factor-1α (HIF-1α) and the pro-angiogenic mediators were decreased in 786-O cells that were transfected with miR-148b-3p mimics. Mechanistically, miR-148b-3p could target fibroblast growth factor-2 (FGF2) and further impaired the activation of fibroblast growth factor receptor 2 (FGFR2). Taken together, our findings demonstrate that miR-148b-3p attenuates renal carcinoma cell growth, the invasion and tube formation of endothelial cell potentially *via* regulating FGF2-FGFR2 signaling pathway.

1. Introduction

Kidney cancer is the ninth most frequent type of cancer and accounts for approximately 3% of adult malignancies worldwide, among which, clear cell renal cell carcinoma (ccRCC) accounts for ~70% [1,2]. As the most common form of kidney tumors, ccRCC is a high-risk metastatic cancer and is also insensitive to chemo/radiotherapies and targeted therapeutic options [3,4]. Therefore, it is urgent to identify novel functional genes and the molecular mechanisms that are involved in the initiation and progression of renal carcinoma. Angiogenesis, the process of formation of new blood vessels from pre-existing vessels or endothelial cell progenitors, plays vital roles in both physiological and pathological progression [5–9]. Angiogenesis is indispensable for tumor growth, clinical drug resistance and metastasis and it has been described as one of the hallmarks of cancer [10,11]. Multiple pro-angiogenic factors and inflammatory cytokines, including vascular endothelial growth factor A (VEGF-A), platelet-derived growth factor (PDGF), placental growth factor (PGF), angiopoietin-1 (Ang-1) and interleukin 6 (IL-6), are involved in tumor angiogenesis [12]. It has been demonstrated that platelet-derived growth factor D (PDGF-D) increases tumor growth and aggressiveness by activating Notch homolog 1 (Notch1) and nuclear factor kappa-light-chain-enhancer of activated B cells (NF-κB) in breast and pancreatic cancer [13,14]. In addition, PDGF-BB is frequently over-expressed in various tumor tissues. PDGF-BB has been found to play important roles in the acquisition of the epithelial-mesenchymal transition (EMT) phenotype of cancer cell and tumor angiogenesis [15]. Meanwhile, a large number of transcriptional factors are closely related with tumor angiogenesis. For instance, as a master regulator of the transcriptional response of angiogenesis, hypoxia-inducible factor 1α (HIF-1α) regulates numerous vital angiogenic genes, such as VEGF and PDGF [16–19]. In addition, many signaling pathways participate in tumor angiogenesis. For example, fibroblast growth factor 2/fibroblast growth factor receptor 2 (FGF2/FGFR2) signaling pathway plays a critical role in promoting basement membrane remodeling, tip cell migration and stalk cell proliferation [20]. Targeting angiogenesis has been supposed to be a therapeutic method for quite a few cancers including renal carcinoma [21,22].By binding to complementary binding sites within the 3′-untranslated region (3′-UTR)

* Corresponding author.
E-mail address: yeqingyqing@sohu.com (Q. Ye).
[1] These authors contributed equally to this work.

https://doi.org/10.1016/j.biopha.2018.07.054
Received 3 April 2018; Received in revised form 9 July 2018; Accepted 10 July 2018

of target mRNAs, miRNAs inhibit the translation of mRNAs or promote their degradation [23]. Functionally, cancer-associated miRNAs control tumor cell growth, invasion, migration and metastasis [24,25]. Lots of evidences have demonstrated that miRNAs could modulate the development of tumor angiogenesis by targeting different angiogenic factors and signaling pathways. For instance, miR-93 promotes tumor angiogenesis by enhancing endothelial cells proliferation, migration and tube formation [26]. MiR-126 may fine-tune angiogenic responses by targeting multiple signaling pathways [27]. Hence, investigations of molecular mechanisms underlying the miRNAs-regulated tumor angiogenesis are essential for improving the outcomes of patients with cancer.

MiR-148b-3p has been found as a tumor-suppressor in numerous types of cancers, including gastric cancer and breast cancer [28,29]. In glioma, miR-148b-3p inhibits the biological activities of glioma cell *via* targeting HOX Transcript Antisense RNA (HOTAIR) [30]. In addition, miR-148b-3p is proved to be capable of inducing cell apoptosis by triggering of caspase-3 and caspase-9 activation, inducing S phase arrest by synchronizing cyclin D1 and p21, and restraining cell invasion in hepatocellular carcinoma [31]. In the present study, we demonstrated that miR-148b-3p not only suppressed renal carcinoma tumor growth but also attenuated the invasion and tube formation of human umbilical vein endothelial cells (HUVECs) through regulating the FGF2/FGFR2 signaling pathway.

2. Materials and methods

2.1. Ethics statement

This study was approved by the Ethics Committee (No: 20161009) of Zhangjiagang Hospital of traditional Chinese Medicine, Jiangsu Province, China. Written consent was obtained from all participants who were involved in the study. All procedures involving experimental animals were performed in accordance with protocols that were approved by the Committee for Animal Research of Zhangjiagang Hospital of traditional Chinese Medicine and complied with the Guide for the Care and Use of Laboratory Animals (NIH publication No. 86-23, revised 1985).

2.2. Cell lines

An immortalized proximal tubule epithelial cell line derived from normal kidney, HK-2, HUVECs and renal carcinoma cell lines (786-O, A-498 and OS-RC-2) were obtained from Nanjing Cobioer Biotechnology Co., Ltd (Nanjing, Jiangsu, China).HK-2 cells were cultured in Keratinocyte Serum Free Medium Kit (17005-042, Invitrogen, Carlsbad, CA, USA). 786-O and OS-RC-2 cells were cultured in RPMI-1640 medium supplemented with 10% FBS, 100 μg/ml penicillin, and 100 μg/ml streptomycin. HUVECs and A-498 cells were cultured in Eagle's Minimum Essential Medium (EMEM) supplemented with 10% FBS, 100 μg/ml penicillin, and 100 μg/ml streptomycin. All cells were maintained in the humidified atmosphere of 5% CO_2 at37 °C. NSC12 (a FGF2/FGFR2 interaction inhibitor) was purchased from Selleck Chemicals (#S7940, Selleck, Texas, USA)

2.3. Clinical tissues

56 cases of renal carcinoma tissues and 23 cases of normal tissues were obtained from the Zhangjiagang Hospital of Traditional Chinese Medicine who underwent surgical treatment between January 1, 2012 and May 30, 2017. The written informed consents for participations in the study were obtained from all patients. Parts of tissue samples were immediately snap-frozen in liquid nitrogen, and parts were fixed in formalin for histological examination.

2.4. Cell transfection

After cultivating in six-well plates at 2×10^5 per well, the cells were subsequently transfected with concentration of 100 nM or 50 nM of miR-185 mimics, or negative control miRNA (miR-NC) (Invitrogen, Carlsbad, CA, USA) for 24 h using Lipofectamine 2000 (#11668019, Invitrogen) according to the instruction manual. For inhibiting the level of miR-148b-3p, cells were transfected with 100 nM miR-148b-3p inhibitor (miR-148b-3p^{inhi}) using Lipofectamine 2000 (#11668019, Invitrogen). MiR-185 mimics, negative control miRNA (miR-NC) and miR-148b-3p inhibitor (miR-148b-3p^{inhi}) were purchased from GenePharma (Shanghai, China). The expression construct of FGF2 was produced by subcloning PCR-amplified full-length human FGF2 complementary DNA (cDNA) into the pcDNA3.1 vector (pcDNA3.1-FGF2). Cells were transfected with pcDNA3.1-FGF2 (0.1 μg/well for 96 well culture plates and 2 μg/well for 6 well culture plates). In co-transfection, miR-148b-3p mimics transfected cells were transfected with pcDNA3.1-FGF2 or empty vector (used as a negative control) for 24 h. After that, the proliferation, migration and invasion assays of the transfected cells were conducted.

2.5. 3-(4,5-dimethyl-2-thiazolyl)-2,5-diphenyl-2-H-tetrazolium bromide (MTT) assay

Cells (2×10^4) were seeded into 96-well plates and were cultured for 24 h, 48 h, 72 h or 96 h, respectively. 10 μl of MTT solution (#G4000, Promega, Madison, WI, USA) was added into 96-well plates. The purple formazan crystal was dissolved in 200 μl dimethylsulfoxide (DMSO) and the optical density (OD) value was measured at 490 nm.

2.6. Colony formation assay

1000 cells/well cells were cultured in 6 well culture plates for 4 weeks [32]. Then, cell colonies were stained with crystal violet and the number of cell colonies was counted.

2.7. Tube formation assay

3×10^4 HUVECs were seeded into 48-well plate that has been precoated with reduced growth factor basement membrane matrix (50 μl/well, #A1413201, Invitrogen). After culturing for 24 h with conditioned media, the total pipe length of the tube-like structure was calculated using image-Pro Plus software. Tracks of HUVECs organised into networks of cellular cords were counted in 5 randomly selected view fields. The tube formation indexes were expressed as tube length (mm)/mm^2 area [33].

2.8. Wound healing assay

Cells were seeded into six-well and were treated with 10 μg/ml Mitomycin C (#BP25312, Fisher Scientific, Hampton, NH, USA) for 2 h to eliminate proliferation. Next, confluent monolayer was scratched using a pipette tip and cells were cultured with conditioned media for 24 h. The area of cell-free scratch was photographed at 0 h and 24 h after scratching. The wound healing effect was determined by measuring the percentage of the remaining cell-free area compared with the area of the initial wound.

2.9. Transwell invasion assay

2×10^3 HUVECs in 100 μl basic media was placed into the upper chamber of an insert (#353097, BD Biosciences, Franklin Lakes, NJ, USA) in a 24-well plate (8 μM pore size), and 500 μl conditioned media derived from 786-O cells was added into the lower chamber. 24 h later, cells on the surface of the membrane were removed using a cotton swap, while invaded cells on the bottom side of membrane were stained

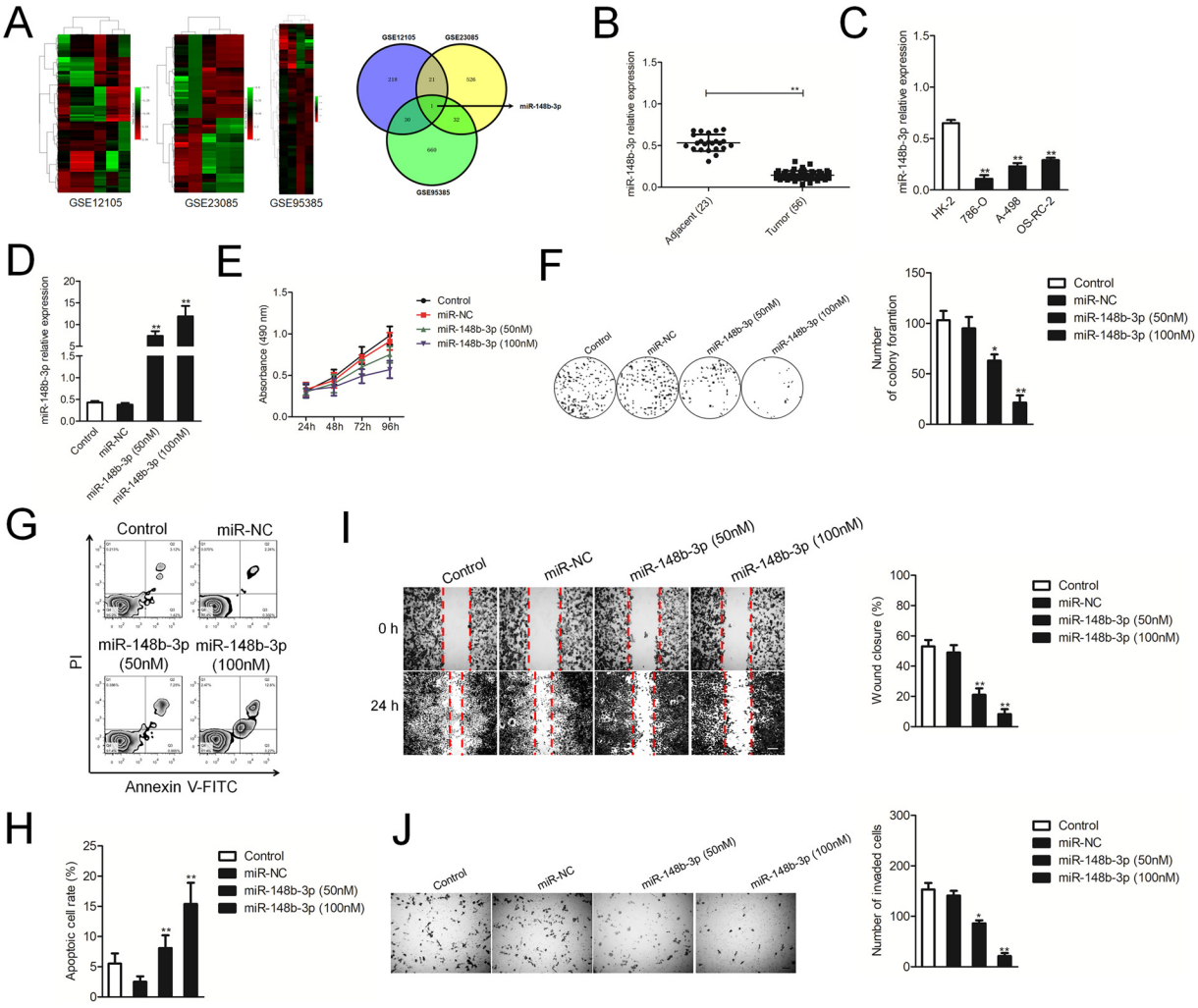

Fig. 1. Over-expression of miR-148b-3p suppresses the proliferation, migration and invasion of 786-O renal carcinoma cell. (A) Analysis of the dysexpression of miRNAs in renal carcinoma tissues and paired normal tissues using three microarray databases (GSE12105, GSE23085 and GSE95385). (B) Total RNAs were abstracted from renal carcinoma tissues and the levels of miR-148b-3p were investigated. $^{**}P < 0.01$, compared to adjacent normal tissues. (C) The levels of miR-148b-3p in HK-2 cells and renal carcinoma cell lines (786-O, A-498 and OS-RC-2) were detected using qRT-PCR assay. $^{**}P < 0.01$ compared to HK-2 cell (D) The level of miR-148b-3p in 786-O cells that were transfected with miR-148b-3p mimics (50 nM or 100 nM) was analyzed by qRT-PCR. $^{**}P < 0.01$, compared to control. (E) The cell viability of 786-O cells that were transfected with miR-148b-3p mimics was determined by MTT assay. (F) Colony formation was conducted to determine the colony formation of 786-O cells that were transfected with miR-148b-3p. (G–H) Annexin V-propidium iodide (PI) double staining was applied to determine the apoptosis of miR-148b-3p over-expressing 786-O cell. (I) Wound healing assay was conducted using miR-148b-3p over-expressing 786-O cell. (J) The invasion of 786-O cells that were transfected with miR-148b-3p mimics was determined by Transwell invasion assay. $^{**}P < 0.01$, compared to control.

with 1% crystal violet and counted under an inverted microscope (CarlZeiss, Hallbergnoos, Germany) at random five fields.

2.10. Enzyme-linked immuno sorbent assay (ELISA) assay

Cells (1×10^5) were cultured in 6-well plates for 24 h. The conditioned medium was collected and the levels of VEGF-A (#ab100662), PDGF-BB (#ab100624) and FGF2 (#ab99979) were detected by commercial enzyme-linked immunosorbent assay (ELISA) kits (Abcam, Cambridge, MA, USA) according to the instruction manual.

2.11. Western blot and real-time quantitative PCR assays

Western blot was carried out as described previously [34]. The anti-HIF-1α (#sc-13515), anti-FGF2 (#sc-136255), anti-VEGF-A (#sc-152) and anti-GAPDH (#sc-32233) were obtained from Santa Cruz (Santa Cruz, CA, USA). The phospho-FGFR2 (Ser782) antibody (#PA5-64796) was purchased from Invitrogen (Carlsbad, CA, USA). RNAs were isolated from renal carcinoma tissues or cells using TRIzol reagent (#15596018, Invitrogen, Carlsbad, CA, USA). First-strand complementary DNA (cDNA) was synthesized with 1 μg RNA using a PrimeScript RT reagent kit (#RR047 A, TakaraBio, Tokyo, Japan). qRT-PCR was performed using IQTM SYBR Green supermix and the ABI 7300 PCR system. The comparative cycle threshold (Ct) method was applied to quantify the expression levels through calculating the $2^{(-\Delta\Delta Ct)}$ method. The primers were synthesis by GenePharma (Shanghai, China). The primers used for PCR were as follows: HIF-1α, (Forward): 5′-GAACGTCGAAAAGAAAAGTCTCG-3′, (Reverse): 5′-CCT TATCAAGATGCGAACTCACA-3′. FGF2: (Forward): 5′-AGAAGAGCGAC CCTCACATCA-3′, (Reverse): 5′-CGGTTAGCACACACTCCTTTG-3′. VEGF-A, (Forward): 5′-AGGGCAGAATCATCACGAAGT-3′, (Reverse): 5′-AGGGTCTCGATTGGATGGCA-3′. PDGF-BB, (Forward): 5′-CTCGATC CGCTCCTTTGATGA-3′ (Reverse): 5′-CGTTGGTGCGGTCTATGAG-3′. PDGF-D: (Forward): 5′-TTGTACCGAAGAGATGAGACCA-3′, (Reverse): 5′-GCTGTATCCGTGTATTCTCCTGA-3′. Glyceraldehyde-3-phosphate dehydrogenase (GAPDH): (Forward): 5′-GGAGCGAGATCCCTCCAA AAT-3′, (Reverse): 5′-GGCTGTTGTCATACTTCTCATGG-3′. Reverse transcription of miR-148b-3p or endogenous control of the small

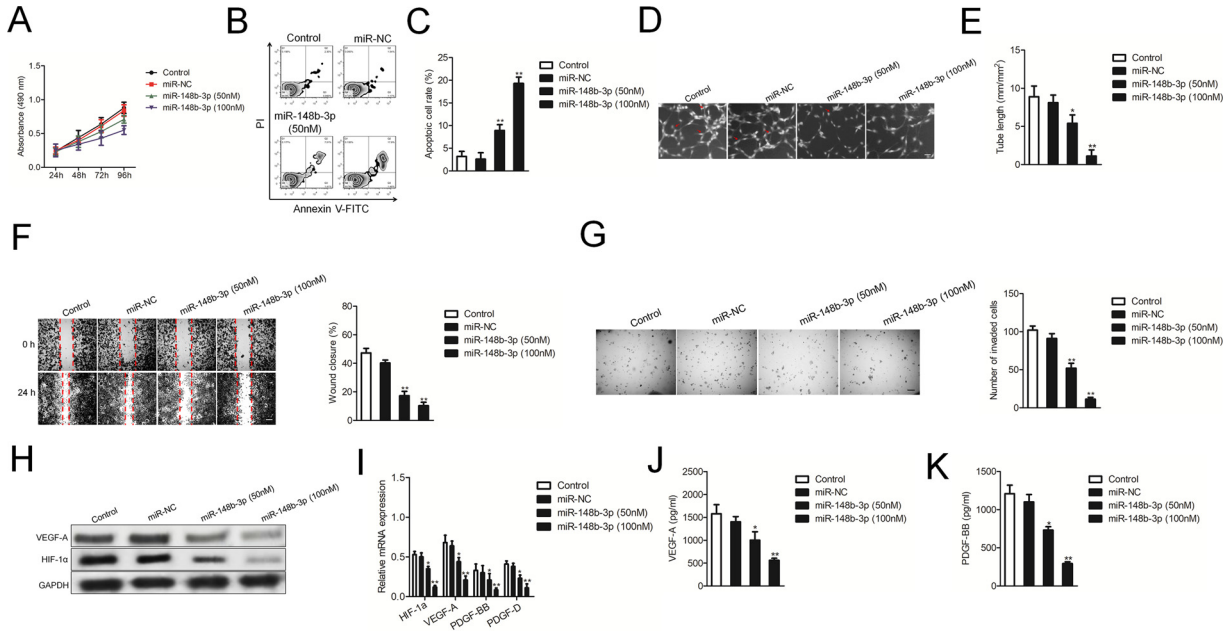

Fig. 2. Over-expression of miR-148b-3p in 786-O cells suppresses the tube formation, migration and invasion of HUVECs. (A) Cell proliferation assays were conducted in HUVECs that were treated with conditioned media derived from miR-148b-3p over-expressing 786-O cells or media derived from control 786-O cells. (B–C) After treated with conditioned media derived from miR-148b-3p over-expressing 786-O cells or media derived from control 786-O cells. HUVECs were collected and stained with Annexin V-FITC and propidium iodide (PI), and the apoptosis was determined by flow cytometry. (D–E) Tube formation assay of HUVECs that were treated with conditioned media derived from 786-O cells. (F–G) Wound healing and Transwell invasion assays were conducted in HUVECs that were treated with conditioned media derived from 786-O cells. (H) The expressions of HIF-1α and VEGF-A in 786-O cell were detected using western blot assay. (I) The mRNA levels of HIF-1α, VEGF-A, PDGF-BB, and PDGF-D in miR-148b-3p over-expressing 786-O cell were analyzed by qRT-PCR. (J–K) The secretions of VEGF-A and PDGF-BB in culture media of 786-O cell were examined by ELISA. * $P < 0.05$, ** $P < 0.01$, compared to control.

nuclear U6 was performed by using total RNA with stem-loop RT-specific primers, and the sequences were as follows: miR-148-3p: 5′-CTC ACATGGTGTCGTGGAGTCGGCTTAACAGTTGAGTACCAAGTT-3′; U6: 5′-CGCTTCACGAATTTGCGTGTCAT-3′.

2.12. Apoptosis assay

HUVECs were washed with PBS and re-suspended in 100 µl 1X staining buffer (a density of 1×10^5) containing FITC-Annexin V and propidium iodide (PI) using a FITC Annexin V apoptosis detection kit (#A9210, Merck KGaA, Darmstadt, Germany) for 15 min. Stained cells were analyzed by flow cytometry with the BD FACS Calibur flow cytometer (BD Biosciences). Three independent experiments were conducted in triplicates.

2.13. Immunofluorescence staining

Cells on glass coverslips were permeabilized in 0.1% Triton X-100. Then, the cells were immunostained by incubating with rabbit monoclonal antibody against FGF2 (#ab92337 1:200, Abcam, Cambridge, MA, USA) at 4 °C for overnight. Then, cells were incubated with FITC-conjugated secondary antibody (#BA1112, 1:100, Boster Biotechnology, Nanjing, Jiangsu, China). Nuclei were then stained using 4′,6-diamidino-2-phenylindole (DAPI) (#AR1177, Boster Biotechnology, Nanjing, Jiangsu, China).

2.14. Luciferase reporter assay

The wild-type 3′-untranslated region (3′-UTR) of FGF2 was named as WT. Site-directed mutagenesis of the miR-148b-3p binding site in the FGF2 3′-UTR was carried out using the GeneTailor Site-Directed Mutagenesis System (#12397-014, Invitrogen) and named mutant type (MUT) 3′-UTR. The WT or MUT FGF2 3′-UTR was cloned into pRL-CMV luciferase reporter (#E2261, Promega, Madison, Wis, USA) and named as pRL-CMV-FGF2. After cultured in 24-well plates, 786-O cells were then transfected with 0.1 µg/well pRL-CMV-FGF2 luciferase reporter combination with miR-148b-3p. And 24 h later, the luciferase activity was detected using the dual-luciferase reporter assay system (Promega, Madison, WI, USA).

2.15. Xenograft assay

Female BALB/c nude mice at 6–8 weeks old (15–20 g) were purchased from Shanghai SLAC Laboratory Animal Co. Ltd. (Shanghai, China). Mice were maintained at dark/light cycles of 12 h duration with food and water available *ad libitum*. 5×10^6 miR-NC or miR-148b-3p transfected cells were subcutaneously inoculated into the nude mice (9 weeks old, n = 6 for each group). The length and width of the resulting tumors (in millimeters) were measured every week with calipers. The tumor diameter was measured, and the volume (length × width^2 × 0.5) was calculated. After 42 days, all mice were sacrificed using CO_2 asphyxiation and then the tumors were removed and the weights of tumors were measured.

2.16. Statistical analysis

Data were presented as Mean ± standard deviation (SD) of three independent experimentations and calculated by SPSS 17.0 statistical software (SPSS, Chicago, IL, USA). Differences in the results of two groups were evaluated using either two-tailed Student's *t*-test or one-way ANOVA followed by post hoc Dunnett's test. $P < 0.05$ was considered as statistically significant.

3. Results

3.1. MiR-148b-3p is down-regulated in renal carcinoma tissues

In order to explore the dysexpression pattern of miRNAs in renal

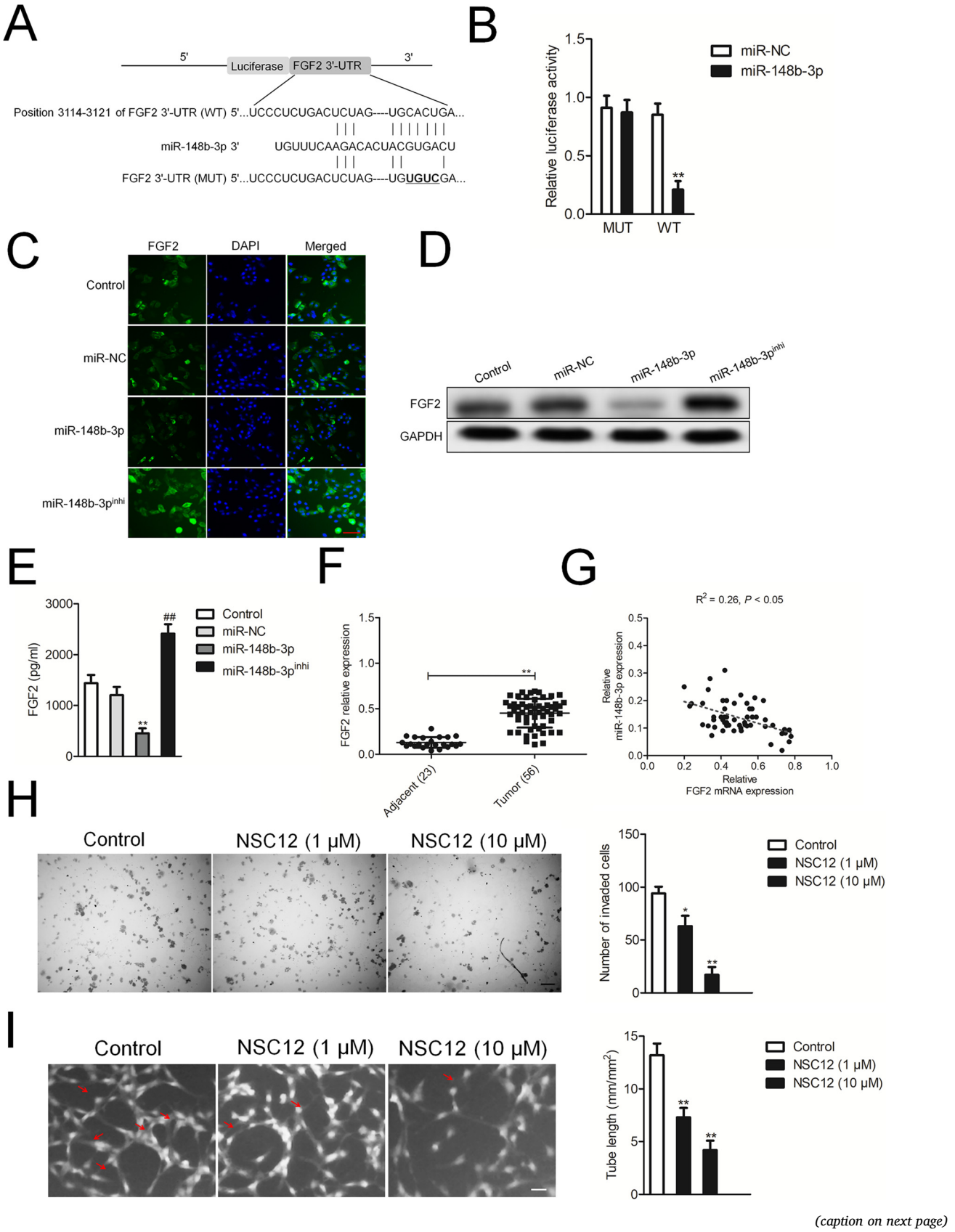

(caption on next page)

carcinoma, three microarray datasets (GSE12105, GSE23085 and GSE95385) were analyzed. MiR-148b-3p, whose function still remains unidentified, was extraordinarily down-regulated in renal carcinoma in comparison with the paired normal tissues (Fig. 1A). To confirm this finding, the levels of miR-148b-3p were analyzed in 56 cases of renal carcinoma tissues and 23 cases of normal tissues. As shown in Fig. 1B, miR-148b-3p was significantly down-regulated in tumor tissues compared to normal tissues as assessed by qRT-PCR assay (Fig. 1B). In

Fig. 3. FGF2 is a direct target of miR-148b-3p in renal carcinoma. (A) Representation of the binding sites between miR-148b-3p and the3′-UTR of FGF2 based on the Targetscan analysis. (B) Luciferase reporter assays using 786-O cells that were cotransfected with 3′-UTR of FGF2 and miR-148b-3p. ** $P < 0.01$, compared to miR-NC. (C–D) The expression of FGF2in 786-O cells was determined by immunofluorescence staining and western blot assays. (E) The level of FGF2 in the culture media of 786-O cell was determined using ELISA assay. ** $P < 0.01$, compared to control. (F) qRT-PCR analysis of FGF2 in renal carcinoma tissues and adjacent normal tissues. ** $P < 0.01$, compared to adjacent normal tissues. (G) The relationship between miR-148b-3p and FGF2 in renal carcinoma tissues was determined using qRT-PCR assay. (H) 786-O cells were treated with or without NSC12. Medium derived from 786-O cells was collected and applied for HUVECs invasion assay in. (I) 786-O cells were treated with or without NSC12 for 24 h, and the medium derived from 786-O cells was collected and applied for HUVECs tube formation assay. ** $P < 0.01$, compared to control.

addition, the qRT-PCR assay indicated that the level of miR-148b-3p was lower in 786-O, A-498 and OS-RC-2 cells than that in the immortalized proximal tubule epithelial cell line, HK-2(Fig. 1C). To investigate the suppressive role of miR-148b-3p, 786-O cells were transfected with miR-148b-3p mimics (Fig. 1D) and the cell growth was determined by MTT and colony formation assay. These results showed that over-expression of miR-148b-3p significantly suppressed the proliferation and colony formation of 786-O cells (Fig. 1E-1 F). Moreover, miR-148b-3p transfection greatly induced the apoptosis of 786-O cells (Fig. 1G-1 H). Next, the wound healing assay and Transwell assay were applied to detect the impact of miR-148b-3p on the migration and invasion of 786-O cells. As expected, miR-148b-3p drastically restrained the migration and invasion of 786-O cell (Fig. 1I–J). All these findings indicated that miR-148b-3p was down-expressed in renal carcinoma and over-expression of mi-148b-3p inhibited renal carcinoma cell growth, migration and invasion *in vitro*.

3.2. Ectopic expression of miR-148b-3p in 786-O cell attenuates HUVECs growth, migration and tube formation

To investigate the function of miR-148b-3p on endothelial cells, we collected the culture media from miR-148b-3p overexpressing 786-O cells and found that media derived from miR-148b-3p overexpressing 786-O cells significantly suppressed HUVECs growth compared with the control media (EMEM) (Fig. 2A). Meanwhile, media derived from miR-148b-3p overexpressing 786-O cells induced the apoptosis of HUVECs (Fig. 2B–C). To evaluate the role of miR-148b-3p in the tube formation of HUVECs, the tube formation assay was conducted. As shown in Fig. 2D–E, conditioned media derived from miR-148b-3p over-expressing 786-O cells significantly decreased the tube length of HUVECs (). Meanwhile, we also performed wound healing and Transwell assays to analysis the effect of miR-148b-3p on HUVECs migration and invasion. Conditioned media derived from miR-148b-3p over-expressing 786-O cells obviously suppressed the migration and invasion abilities of HUVECs (Fig. 2F–G). Next, we performed qRT-PCR and immunoblotting to test the expressions of HIF-1α and VEGF-A in miR-148b-3p over-expressed 786-O cells. Over-expression of miR-148b-3p in 786-O cells decreased the mRNA levels of HIF-1a, VEGF-A, PDGF-BB, and PDGF-D, and suppressed the protein levels of HIF-1α and VEGF-A (Fig. 2H–I). Importantly, miR-148b-3p decreased the levels of VEGF-A and PDGF-BB in the culture media of 786-O cells (Fig. 2J–K). All these results indicated that miR-148b-3p might suppress the growth, migration, invasion and tube formation of HUVECs as well as enhance their apoptosis.

3.3. FGF2 is direct target of miR-148b-3p in renal carcinoma

To determine the fundamental mechanisms of miR-148b-3p, we performed a bioinformatics analysis using Targetscan (http://www.targetscan.org/vert_71/) to predict the target genes of miR-148b-3p. We found that the 3′-UTR of FGF2 contained theoretical binding sites on miR-148b-3p (Fig. 3A). To study whether FGF2 might be a direct target of miR-148b-3, we performed a luciferase reporter assay in 786-O cell. Over-expression of miR-148b-3p suppressed the luciferase activity of wild type (WT) FGF2 3′-UTR, but failed to inhibit the luciferase activity of mutant type (MUT) FGF2 3′-UTR (Fig. 3B). Additionally, miR-148b-3p significantly inhibited the protein level of FGF2 whereas miR-148b-3p inhibitor (miR-148b-3p^{inhi}) transfected in 786-O cells remarkably increased the level of FGF2, as demonstrated by the immunofluorescence staining and western blot assays (Fig. 3C-D). Consistently, miR-148b-3p decreased the secretion of FGF2 and miR-148b-3p^{inhi} transfected markedly increased the secretion of FGF2 in the culture media of 786-O cell (Fig. 3E). qRT-PCR analysis also revealed that the expression of FGF2 was higher in the 56 analyzed cases of renal carcinoma tissues compared to 23 cases of normal tissues (Fig. 3F). Importantly, negatively relationship between FGF2 and miR-148b-3 was also found in renal carcinoma tissues (Fig. 3G). These results demonstrated that the endogenous FGF2 was directly targeted by miR-148b-3p. To further test whether inhibition of FGF2-FGFR2 pathway could impair the invasion and tube formation of endothelial cells, we treated 786-O cells with 1 μM or 10 μM NSC12 (a FGF2/FGFR2 interaction inhibitor) and medium from NSC12 treated 786-O cells was collected and applied for Transwell invasion assay and tube formation in HUVECs [35,36]. We found that medium derived from NSC12 treated 786-O cells prevented the invasion and tube formation of HUVECs *in vitro* (Fig. 3H-3I).

3.4. MiR-148b-3p reduces the growth of renal carcinoma cell and suppresses the expression of FGF2 in vivo

Finally, we sought to determine whether miR-148b-3p could affect the growth of renal carcinoma cell in nude mouse model *in vivo*. 786-O cells were transfected with either miR-NC or miR-148b-3p, and then were implanted subcutaneously into nude mice. Consistent with the *in vitro* findings, the tumor growth was significantly inhibited in nude mice that were implanted miR-148b-3p overexpressing 786-O cells (Fig. 4A-B). Next, we determined the expression levels of FGF2 and of p-FGFR2 in these tumors using immunohistochemical (IHC) staining. The tumors that derived from miR-148b-3p overexpressing 786-O cells had lower levels of FGF2 and p-FGFR2 than the tumors that derived from miR-NC transfection 786-O cells (Fig. 4C). We next explored whether over-expression of FGF2 could reverse the inhibitory effects of miR-148b-3p on 786-O cell proliferation, migration and invasion. 786-O cell was co-transfected with miR-148b-3p and pcDNA3.1-FGF2. The mRNA level of FGF2 in 786-O cells was quantified using qRT-PCR assay (Fig. 4D). Then, MTT and colony formation experiments were conducted to detect whether pcDNA3.1-FGF2 reversed the inhibitory effect of miR-148b-3p on 786-O cell growth. As shown in Fig. 4E-F, up-regulation of FGF2 reversed the inhibitory impacts of miR-148b-3p on the proliferation and colony formation of 786-O cell. Consistently, cells that were transfected with FGF2 restored the migration and invasion abilities in the presence miR-148b-3p (Fig. 4G-H). Finally, we assessed whether the over-expression of FGF2 could rescue the inhibitory effects of miR-148b-3p on the tube formation and invasion of HUVECs. As shown in Fig. 4I-J, conditioned media derived from miR-148b-3p over-expressing 786-O cells significantly decreased the tube formation and invasion of HUVECs whereas up-regulation of FGF2 in miR-148b-3p mimics transfected 786-O cells rescued the tube formation and invasion of HUVECs *in vitro*. All these results suggested that miR-148b-3p influenced the growth of renal carcinoma cell, the invasion as well as the tube formation of HUVECs by targeting FGF2.

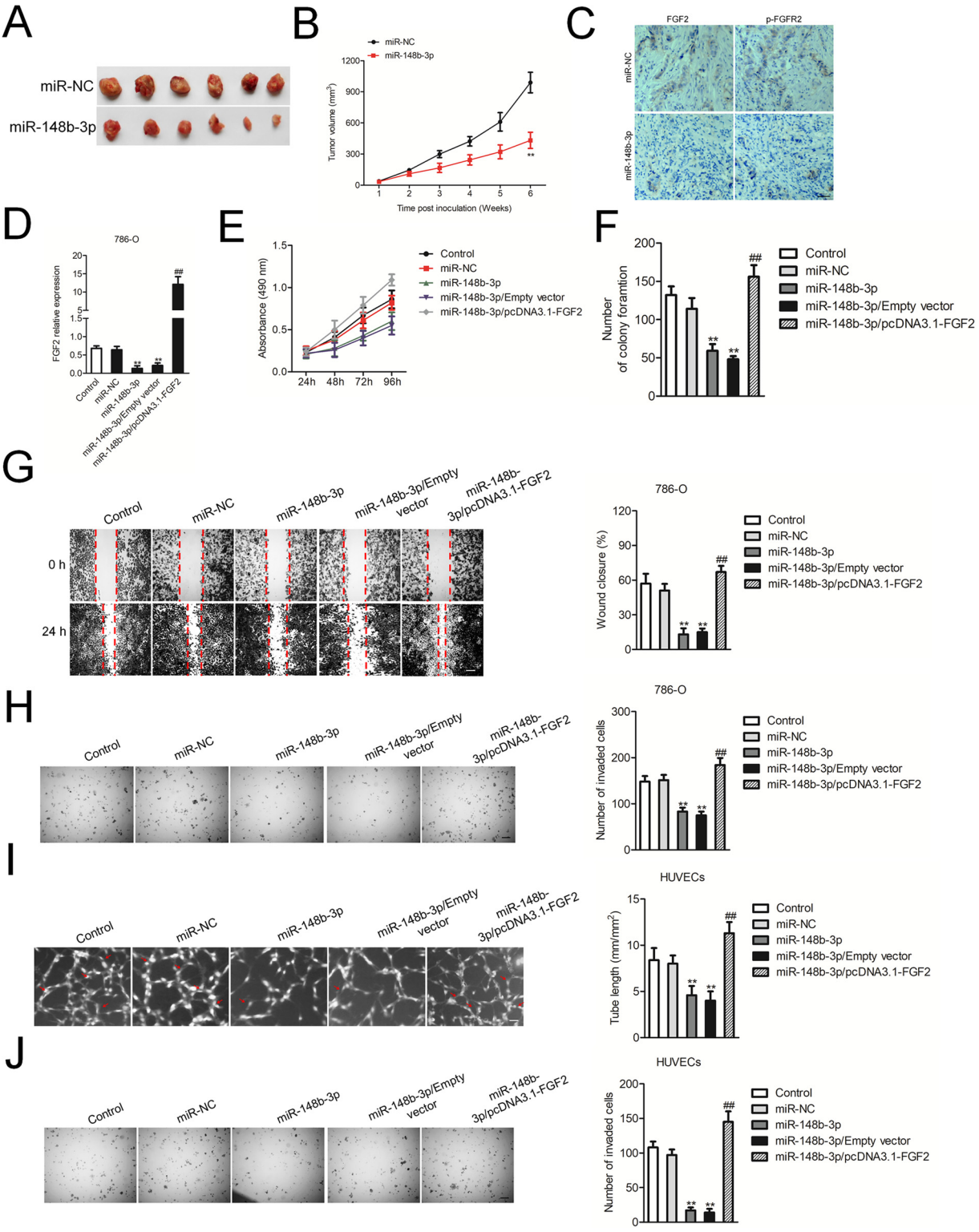

Fig. 4. FGF2-FGFR2 is involved in the inhibitory effect of miR-148b-3p on renal carcinoma cell. (A) Representative picture of xenograft tumors that derived from miR-NC or miR-148b-3p transfected 786-O cells. (B) Tumor volumes in two groups were measured at each week. ** $P < 0.01$, compared to miR-NC. (C) The expressions of FGF2 and p-FGFR2 in the xenograft tumors were determined by IHC staining. (D) 786-O cells were transfected with miR-148b-3p alone or co-transfected with pcDNA3.1-FGF2 and miR-148b-3p. The expression of FGF2 was determined by qRT-PCR assay. (E) 786-O cell was transfected with miR-148b-3p alone, or co-transfected with pcDNA3.1-FGF2 and miR-148b-3p, and then was seeded into 96 well plates. After 24 h, 48 h, 72 h and 96 h, the MTT assay was conducted to analyze cell proliferation. (F) Colony formation assay of 786-O cells. Representative images for each treatment are shown. (G) 786-O cells were transfected with miR-148b-3p alone, or co-transfected with pcDNA3.1-FGF2 and miR-148b-3p. Then, cells were subjected to wound healing assay. Scale bar: 200 μm. (H) Transwell invasion assay was conducted in 786-O cells that were transfected with miR-148b-3p alone, or co-transfected with pcDNA3.1-FGF2 and miR-148b-3p. Scale bar: 200 μm. (I) Conditioned medium derived from 786-O cells that were transfected with miR-148b-3p alone, or co-transfected with pcDNA3.1-FGF2 and miR-148b-3p was collected. Tube formation assays of HUVECs that were treated with conditioned media. (J) Transwell invasion assay of HUVECs that were treated with conditioned media derived from 786-O cells. ** $P < 0.01$, compared to control; $^{\#\#}$ $P < 0.01$, compared to miR-148b-3p.

4. Discussion

In this research, a series of analyses using miR-148b-3p over-expressing renal carcinoma cell were conducted and the results suggested the suppressive roles of miR-148b-3p in renal carcinoma cell growth and pro-angiogenic phenotype of HUVECs. First, microRNA arrays analysis demonstrated that miR-148b-3p was significantly down-regulated in renal carcinoma, and over-expression of miR-148b-3p suppressed the proliferation and aggressiveness of renal carcinoma 786-O cell *in vitro*. These results were in accordance with the previously studies [31,37], in which miR-148b serves as a tumor suppressor in hepatocellular carcinoma. Second, conditioned media derived from miR-148b-3p over-expressing 786-O cell decreased the tube formation and invasion abilities and induced the apoptosis of HUVECs. Our study provided the first evidence of the suppressive role of miR-148b-3p in renal carcinoma cell growth and the pro-angiogenic phenotype of HUVECs induced by renal carcinoma cell.

Although the role of miR-148b-3p in renal carcinoma remains mysterious, several genes have been reported to be regulated by miR-148b in cancers, including non-small cell lung cancer (NSCL) [38]. For example, recent research has showed that the miRNA-148b is down-regulated in gastric cancer and serves as a tumor suppressor through targeting cholecystokinin B receptor (CCKBR) [39]. The expression of miR-148b is also down-regulated in human colorectal cancer tissues and miR-148b inhibits colorectal cancer cell growth *in vitro* and *in vivo* [40]. These results are in accordance with our study, in which we found that miR-148b-3p was down-expressed in renal carcinoma tissues and cell lines, in comparison with normal tissues and human renal tubule epithelial cell line.

To understand how miR-148b-3p inhibited the pro-angiogenic phenotype of HUVECs, the well-known angiogenesis associated factors HIF-1α, VEGF-A, and PDGF-BB were analyzed in our study. Our results demonstrated that over-expression of miR-148b-3p suppressed the expression of HIF-1α, VEGF-A, and PDGF-BB in 786-O cell. Moreover, over-expression of miR-148b-3p in 786-O cell inhibited the invasion and tube formation of HUVECs *in vitro*. Another finding of this study was that the FGF2-FGFR2 cascade was potentially involved into the suppressive roles of miR-148b-3p on renal carcinoma cell growth, migration and invasion. MicroRNAs regulate the expression of target genes by inhibiting the translation of mRNAs or promoting their degradation. The potential target of miR-148b-3p was further explored. Using the online prediction tool (http://www.targetscan.org) and the luciferase activity assay, we found that FGF2 was the potential target of miR-148b-3p. In addition, FGF2 was up-regulated in renal carcinoma tissues, and inhibition of FGF2-FGFR2 activity by using NSC12 in 786-O cell suppressed the aggressive phenotypes of 786-O cell and the pro-angiogenic phenotype of HUVECs. Xenografted tumor model was applied for elucidating the role of miR-148b-3p in the growth of renal carcinoma cell *in vivo*. Consistent with the results *in vitro*, miR-148b-3p suppressed renal carcinoma cell growth and inhibited the activity of FGF2/FGFR2 *in vivo*. In conclusion, we demonstrated that up-regulation of miR-148b-3p inhibited renal carcinoma cell growth and the pro-angiogenic phenotype of HUVECs by targeting of FGF2-FGFR2 signaling pathway

Conflicts of interest

We declare no conflict of interest.

Acknowledgement

This study was supported by Suzhou Science and Technology Development Plan (No. SYSD2015182).

References

[1] L. Teng, Y. Chen, Y. Cao, et al., Overexpression of ATP citrate lyase in renal cell carcinoma tissues and its effect on the human renal carcinoma cells in vitro, Oncol. Lett. 15 (2018) 6967–6974.
[2] J. Wang, L. Yuan, X. Liu, et al., Bioinformatics and functional analyses of key genes and pathways in human clear cell renal cell carcinoma, Oncol. Lett. 15 (2018) 9133–9141.
[3] J. Lefebvre, I.G. Glezerman, Kidney toxicities associated with novel Cancer therapies, Adv. Chronic Kidney Dis. 24 (2017) 233–240.
[4] H.C. Arora, M. Fascelli, J.H. Zhang, et al., Kidney, ureteral, and bladder Cancer: A primer for the internist, Med. Clin. North Am. 102 (2018) 231–249.
[5] Y.C. Lin, C.Y. Liu, R. Kannagi, et al., Inhibition of endothelial SCUBE2 (Signal Peptide-CUB-EGF domain-containing protein 2), a novel VEGFR2 (Vascular endothelial growth factor receptor 2) coreceptor, suppresses tumor angiogenesis, Arterioscler. Thromb. Vasc. Biol. 38 (2018) 1202–1215.
[6] L. Zhang, Z. Lv, J. Xu, et al., MicroRNA-134 inhibits osteosarcoma angiogenesis and proliferation by targeting the VEGFA/VEGFR1 pathway, FEBS J. 285 (2018) 1359–1371.
[7] M. Rajabi, S.A. Mousa, The role of angiogenesis in Cancer treatment, Biomedicines 5 (2017) 34.
[8] L.M. Ellis, W. Liu, F. Fan, et al., Role of angiogenesis inhibitors in cancer treatment, Oncology (Williston Park) 15 (2001) 39–46.
[9] T.S. Mafu, A.V. September, D. Shamley, The potential role of angiogenesis in the development of shoulder pain, shoulder dysfunction, and lymphedema after breast cancer treatment, Cancer Manag. Res. 10 (2018) 81–90.
[10] R.N. Gacche, Y.G. Assaraf, Redundant angiogenic signaling and tumor drug resistance, Drug Resist. Update 36 (2018) 47–76.
[11] D. Hanahan, R.A. Weinberg, Hallmarks of cancer: the next generation, Cell 144 (2011) 646–674.
[12] X. Zhou, J. Chen, Q. Xiao, et al., MicroRNA-638 inhibits cell growth and tubule formation by suppressing VEGFA expression in human Ewing sarcoma cells, Biosci. Rep. 38 (2018) BSR20171017.
[13] A. Ahmad, Z. Wang, D. Kong, et al., Platelet-derived growth factor-D contributes to aggressiveness of breast cancer cells by up-regulating Notch and NF-kappaB signaling pathways, Breast Cancer Res. Treat. 126 (2011) 15–25.
[14] Z. Wang, D. Kong, S. Banerjee, et al., Down-regulation of platelet-derived growth factor-D inhibits cell growth and angiogenesis through inactivation of Notch-1 and nuclear factor-kappaB signaling, Cancer Res. 67 (2007) 11377–11385.
[15] L.J. Nissen, R. Cao, E.M. Hedlund, et al., Angiogenic factors FGF2 and PDGF-BB synergistically promote murine tumor neovascularization and metastasis, J. Clin. Invest. 117 (2007) 2766–2777.
[16] J. Dewangan, S. Kaushik, S.K. Rath, et al., Centchroman regulates breast cancer angiogenesis via inhibition of HIF-1alpha/VEGFR2 signalling axis, Life Sci. 193 (2018) 9–19.
[17] A. Ahluwalia, A.S. Tarnawski, Critical role of hypoxia sensor–HIF-1alpha in VEGF gene activation. Implications for angiogenesis and tissue injury healing, Curr. Med. Chem. 19 (2012) 90–97.
[18] S. Unwith, H. Zhao, L. Hennah, et al., The potential role of HIF on tumour progression and dissemination, Int. J. Cancer 136 (2015) 2491–2503.
[19] C.A. Clara, S.K. Marie, J.R. de Almeida, et al., Angiogenesis and expression of PDGF-C, VEGF, CD105 and HIF-1alpha in human glioblastoma, Neuropathology 34 (2014) 343–352.
[20] Y. Hori, K. Ito, S. Hamamichi, et al., Functional characterization of VEGF- and FGF-induced tumor blood vessel models in human Cancer xenografts, Anticancer Res. 37 (2017) 6629–6638.
[21] L. Saes, F. Eskens, Tivozanib: a new treatment option for renal cell carcinoma, Drugs Today 53 (2017) 609–618.
[22] J.E. Frampton, Pazopanib: a review in advanced renal cell carcinoma, Target Oncol. 12 (2017) 543–554.
[23] W.C. Cho, MicroRNAs: potential biomarkers for cancer diagnosis, prognosis and targets for therapy, Int. J. Biochem. Cell Biol. 42 (2010) 1273–1281.
[24] J.M. Bouyssou, S. Manier, D. Huynh, et al., Regulation of microRNAs in cancer metastasis, Biochim. Biophys. Acta 1845 (2014) 255–265.
[25] J. Kim, F. Yao, Z. Xiao, et al., MicroRNAs and metastasis: small RNAs play big roles, Cancer Metastasis Rev. 37 (2018) 5–15.
[26] L. Liang, L. Zhao, Y. Zan, et al., MiR-93-5p enhances growth and angiogenesis capacity of HUVECs by down-regulating EPLIN, Oncotarget 8 (2017) 107033–107043.
[27] C. Shan, Y. Ma, MicroRNA-126/stromal cell-derived factor 1/C-X-C chemokine receptor type 7 signaling pathway promotes post-stroke angiogenesis of endothelial progenitor cell transplantation, Mol. Med. Rep. 17 (2018) 5300–5305.
[28] F. Orso, L. Quirico, F. Virga, et al., miR-214 and miR-148b targeting inhibits dissemination of melanoma and breast Cancer, Cancer Res. 76 (2016) 5151–5162.
[29] X. Ding, J. Liu, T. Liu, et al., miR-148b inhibits glycolysis in gastric cancer through targeting SLC2A1, Cancer Med. 6 (2017) 1301–1310.
[30] G. Wang, Z. Li, N. Tian, et al., miR-148b-3p inhibits malignant biological behaviors of human glioma cells induced by high HOTAIR expression, Oncol. Lett. 12 (2016) 879–886.
[31] J.G. Zhang, Y. Shi, D.F. Hong, et al., MiR-148b suppresses cell proliferation and invasion in hepatocellular carcinoma by targeting WNT1/beta-catenin pathway, Sci. Rep. 5 (2015) 8087.
[32] S. Muniyan, S.J. Chen, F.F. Lin, et al., ErbB-2 signaling plays a critical role in regulating androgen-sensitive and castration-resistant androgen receptor-positive prostate cancer cells, Cell Signal. 27 (2015) 2261–2271.

[33] L. Zhou, H. Chen, X. Mao, et al., G-protein-coupled receptor 30 mediates the effects of estrogen on endothelial cell tube formation in vitro, Int. J. Mol. Med. 39 (2017) 1461–1467.
[34] X.Y. Liu, Y.J. He, Q.H. Yang, et al., Induction of autophagy and apoptosis by miR-148a through the sonic hedgehog signaling pathway in hepatic stellate cells, Am. J. Cancer Res. 5 (2015) 2569–2589.
[35] R. Ronca, A. Giacomini, E. Di Salle, et al., Long-pentraxin 3 derivative as a small-molecule FGF trap for Cancer therapy, Cancer Cell 28 (2015) 225–239.
[36] R. Castelli, A. Giacomini, M. Anselmi, et al., Synthesis, structural elucidation, and biological evaluation of NSC12, an orally available fibroblast growth factor (FGF) ligand trap for the treatment of FGF-Dependent lung tumors, J. Med. Chem. 59 (2016) 4651–4663.
[37] X. Chen, L. Bo, W. Lu, et al., MicroRNA-148b targets Rho-associated protein kinase 1 to inhibit cell proliferation, migration and invasion in hepatocellular carcinoma, Mol. Med. Rep. 13 (2016) 477–482.
[38] G. Zhai, G. Li, B. Xu, et al., miRNA-148b regulates radioresistance in non-small lung cancer cells via regulation of MutL homologue 1, Biosci. Rep. 36 (2016) e00354.
[39] Y.X. Song, Z.Y. Yue, Z.N. Wang, et al., MicroRNA-148b is frequently down-regulated in gastric cancer and acts as a tumor suppressor by inhibiting cell proliferation, Mol. Cancer 10 (2011) 1.
[40] Y. Song, Y. Xu, Z. Wang, et al., MicroRNA-148b suppresses cell growth by targeting cholecystokinin-2 receptor in colorectal cancer, Int. J. Cancer 131 (2012) 1042–1051.